Electronic Supplementary Material (ESI) for CrystEngComm.
This journal is © The Royal Society of Chemistry 2020

A novel cadmium metal-organic framework-based multiresponsive fluorescent sensor demonstrating the outstanding sensitivities and selectivities for detecting NB, Fe^{3+} ions and $Cr_2O_7^{2-}$ anions

Xiuli Wang, Yu Liu, Hongyan Lin, Na Xu,Guocheng Liu, Xiang Wang, Zhihan Chang Jianrong Li

Experimental

Materials and methods

The N-ligand was prepared according to the synthesis method of the literature[1]. All the reagents and solvents used in the experiments were bought commercially. The infrared (IR) spectra data were gathered on a Varian640 FTIR spectrometer through KBr pellet from 500 cm^{-1} to 4000 cm^{-1} region and the powder X-ray diffraction (PXRD) patterns were collected on a D/te X Ultra diffractometer with Mo Kα radiation (λ =0.71073 Å).The fluorescent spectra were recorded on a Hitachi F-4500 luminescence/phosphorescence spectrometer. UV-vis absorption spectra were carried out on Perkin Elmer Lambda 750.

Preparation of $[Cd_3(L)(NTB)_2(DMA)_2]\cdot 2DMA$

The mixture of $Cd(NO_3)_2\cdot 4H_2O$ (30 mg, 0.1 mmol), L ligand (21 mg, 0.05 mmol) and H_3NTB (18 mg, 0.05 mmol) were dissolved in 2.8mL N,N-dimethylacetamide (DMA) and 0.4mL 10^{-2} M HNO_3, which was moved to a 25 mL Teflon vessel within the autoclave. The mixture was heated at 120°C for 4 days and then cooled to room temperature, yellow crystals were obtained as single product (Yield: 71%, based on Cd). Anal. Calcd for $C_{84}H_{80}Cd_3N_{10}O_{18}$: C, 54.39; H, 4.34; N, 7.55. Found: C 54.33; H 4.38; N 7.57. IR (KBr, cm^{-1}): 3431 (m), 1600 (s), 1548 (s), 1509 (m), 1424 (m), 1389 (s), 1315 (m), 1287 (w), 1176 (w), 1107 (w), 1018 (w), 857 (w), 783 (s), 704 (w), 672 (w), 591 (w), 547 (m).

X-Ray crystallography

The single-crystal diffraction data for Cd-MOF was collected on a Bruker SMART APEX II with Mo Kα (λ = 0.71073 Å) by ω and θ scan mode at room temperature. All the structures were solved by direct methods using OLEX program[2]. The crystal data and structure refinement results are summarized in Table S1. Selected bond lengths and angles are listed in Table S2. CCDC 1992610 for Cd-MOF contain the supplementary crystallographic data in this paper. These data can be obtained free of charge from The Cambridge Crystallographic Data Centre *via* www.ccdc.cam.ac.uk/data_request/cif.

The Powder X-ray diffraction (PXRD) and fourier transform infrared (FTIR)

As depicted in Fig. S2a, the experimental PXRD patterns of crystals match well with the simulated ones from crystal structures, indicating good phase purity of the synthesized Cd-MOF. In order to evaluate the stability of Cd-MOF, the PXRD patterns of Cd-MOF in various conditions are performed and match well with their simulated ones, demonstrating the excellent stability of

Cd-MOF in water and DMA solution. The FTIR spectroscopy demonstrates the functional groups of Cd-MOF (Fig. S4). Strong peaks at 1670 and 1506 cm^{-1} can be ascribed to asymmetric and symmetric stretching vibrations of carboxyl groups of H_3NTB[3]. The strong peaks at 1595, 1385 cm^{-1} suggest the amide stretching vibrations of L ligands[4]. Absorption peaks located at 1483, 1427, 1334 cm^{-1} suggest the *v*(C-N) stretching vibrations of the pyridyl rings from L ligands[5].

The thermogravimetric analyses (TGA)

The TG curve is shown in Fig. S5. The first weight loss from 30 to 205 °C corresponds to the removal of two DMA molecules in Cd-MOF. The second weight loss occurs in the temperature range of 205-315°C, which can be attributed to the loss of two coordinated DMA molecules. These two weight loss steps with the total loss 18.6% (cal. 18.7%) can be seen. Then after 460°C, there is a rapid weight loss representing the decomposition of Cd-MOF.

Table S1 Crystallographic data for the title Cd-MOF

Complex	**Cd-MOF**
Empirical formula	$C_{84}H_{80}Cd_3N_{10}O_{18}$
Formula weight	1854.78
Crystal system	Triclinic
Space group	$P\bar{1}$
a (Å)	13.6803(13)
b (Å)	13.8392(13)
c (Å)	14.6811(15)
α (°)	101.399(2)
β (°)	99.384(2)
γ (°)	116.889(2)
V (Å ^{3})	2326.6(4)
Z	1
D_c (g cm^{-3})	1.324
μ (mm^{-1})	0.745
F (000)	942
Reflection collected	17756
Unique reflections	11852
parameters	526
R_{int}	0.0212
GOF	1.047
$R_1{}^a$ [$I > 2\sigma(I)$]	0.0402
$wR_2{}^b$ (all data)	0.1001

$^aR_1 = \sum||F_o| - |F_c||/\sum|F_o|$; $^bwR_2 = \Sigma[w(F_o^2-F_c^2)^2]/\Sigma[w(F_o^2)^2]]^{1/2}$

Table S2. Selected bond distances (Å) and angles (°) for Cd-MOF

$C_{68}H_{44}Cd_3N_6O_{14}$			
Cd(1)-O(1)	2.2120(2)	Cd(1)-O(5)#2	2.302(2)
Cd(1)-O(1)#1	2.2120(2)	Cd(1)-O(5)#3	2.302(2)
Cd(1)-O(3)#4	2.309(2)	Cd(2)-O(5)#6	2.251(2)

Cd(1)-O(3)#5	2.309(2)	Cd(2)-O(2)#7	2.252(2)
Cd(2)-O(4)	2.191(2)	Cd(2)-O(7)	2.390(2)
Cd(2)-O(6)#6	2.538(2)	Cd(2)-N(1)	2.267(3)
O(1)#1-Cd(1)-O(1)	180.0	O(1)-Cd(1)-O(5)#3	87.51(8)
O(1)-Cd(1)-O(5)#2	92.49(8)	O(1)#1-Cd(1)-O(5)#3	92.49(8)
O(1)#1-Cd(1)-O(5)#2	87.51(8)	O(1)-Cd(1)-O(3)#4	86.06(8)
O(1)-Cd(1)-O(3)#5	93.94(8)	O(1)#1-Cd(1)-O(3)#5	86.06(8)
O(1)#1-Cd(1)-O(3)#4	93.94(8)	O(5)#3-Cd(1)-O(5)#2	180.0
O(5)#3-Cd(1)-O(3)#4	91.29(8)	O(5)#2-Cd(1)-O(3)#5	91.29(8)
O(5)#3-Cd(1)-O(3)#5	88.71(8)	O(5)#2-Cd(1)-O(3)#4	88.71(8)
O(3)#4-Cd(1)-O(3)#5	180.0	O(5)#6-Cd(2)-O(2)#7	124.25(10)
O(5)#6-Cd(2)-O(7)	86.51(8)	O(5)#6-Cd(2)-O(6)#6	54.13(7)
O(5)#6-Cd(2)-N(1)	149.12(10)	O(2)#7-Cd(2)-O(7)	174.60(8)
O(2)#7-Cd(2)-O(6)#6	100.04(9)	O(2)#7-Cd(2)-N(1)	88.47(9)
O(4)-Cd(2)-O(5)#6	97.54(9)	O(4)-Cd(2)-O(2)#7	97.01(9)
O(4)-Cd(2)-O(7)	85.51(9)	O(4)-Cd(2)-O(6)#6	148.55(9)
O(4)-Cd(2)-N(1)	111.71(11)	O(7)-Cd(2)-O(6)#6	79.90(9)
N(1)-Cd(2)-O(6)#6	95.03(10)	N(1)-Cd(2)-O(7)	86.16(9)

Symmetry codes: #1 -x,-y+3,-z+2; #2 x-1,y,z; #3 -x+1,-y+3,-z+2; #4 -x,-y+2,-z+2; #5 x,y+1,z; #6 x-1,y-1,z; #7 x,y-1,z

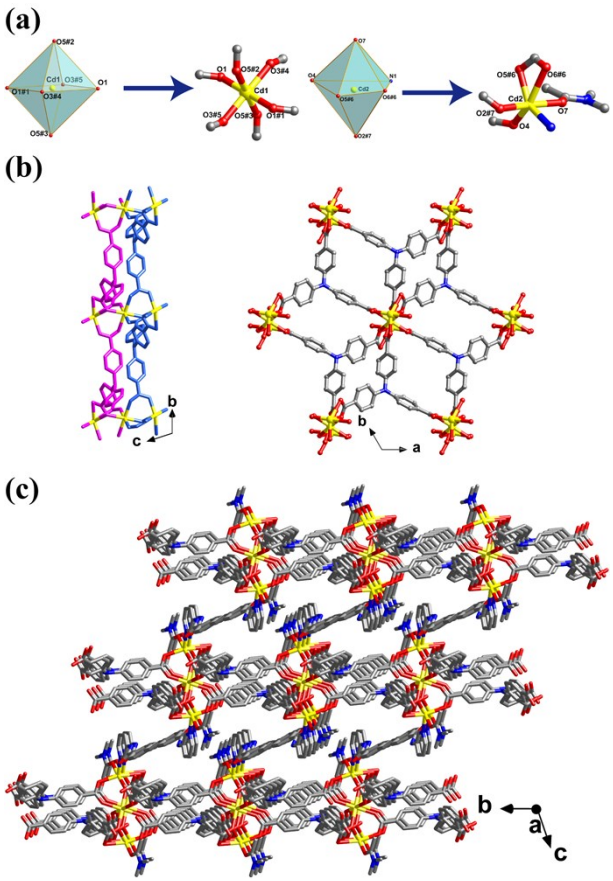

Fig. S1 (a) Coordination configurations of Cd1 and Cd2 ions in the Cd-MOF; (b) The 2D bilayer structure of Cd-MOF; (c) The 3D structure of Cd-MOF.

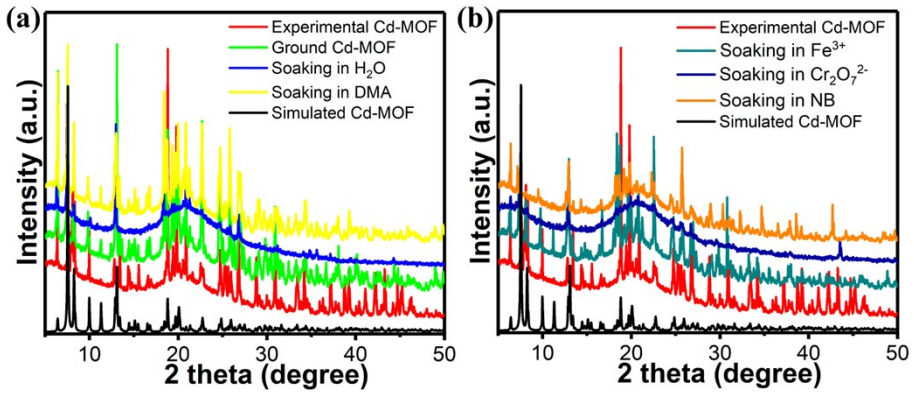

Fig. S2 (a) X-ray powder diffraction patterns of Cd-MOF: simulated (black); as-synthesized (red); ground Cd-MOF (green); soaking in H_2O (blue) and soaking in DMA (yellow); (b) simulated (black); as-synthesized (red); soaking in Fe^{3+} (olive) and soaking in $Cr_2O_7^{2-}$ (royal); soaking in NB (orange).

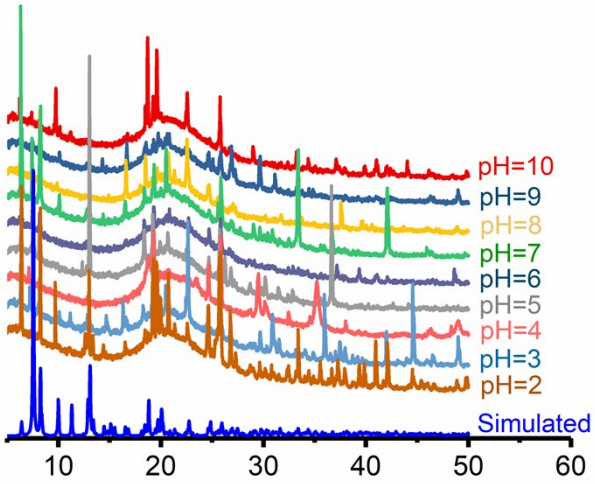

Fig. S3 The PXRD patterns of the Cd-MOF after soaked in aqueous solution of pH 2-10 for 24h.

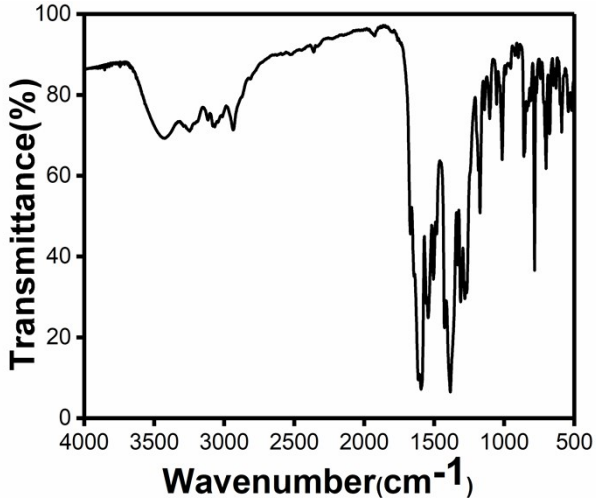

Fig. S4 The IR spectra of Cd-MOF.

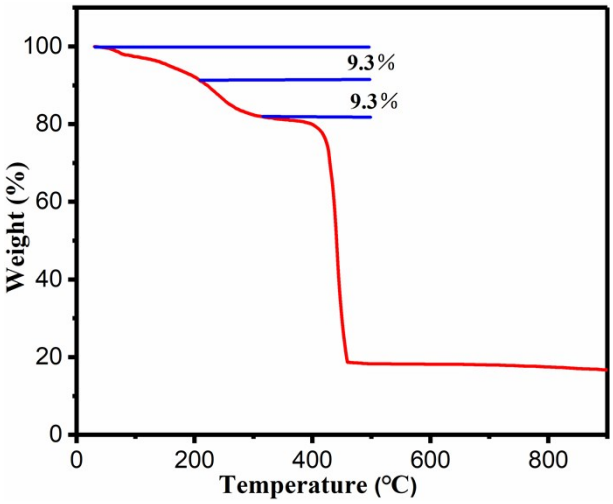

Fig. S5 The TG curve of Cd-MOF

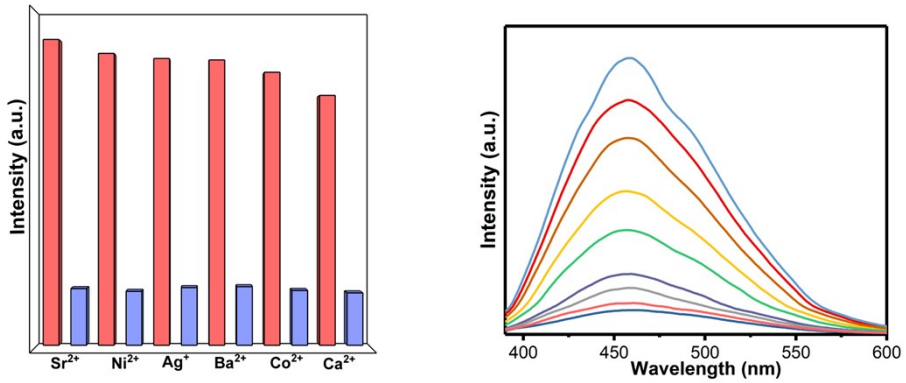

Fig. S6. (a) The effect of other metal ions on the fluorescence intensities of Al^{3+}; (b) Fluorescence spectra of Cd-MOF with Al^{3+} at di□erent concentrations.

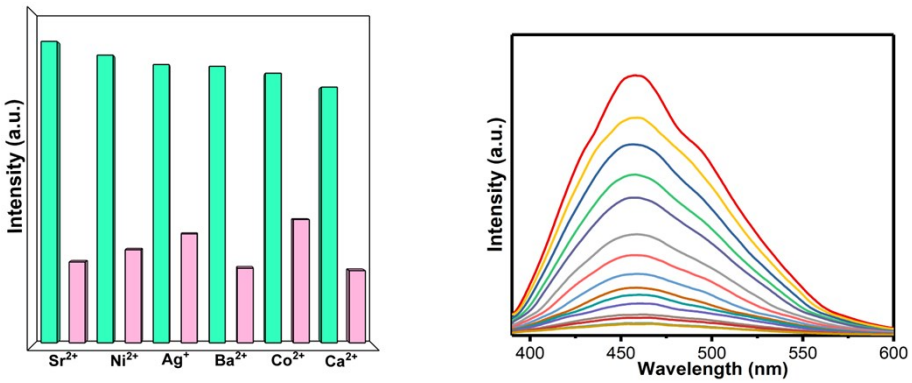

Fig. S7. (a) The effect of other metal ions on the fluorescence intensities of Cu^{2+}; (b) Fluorescence spectra of Cd-MOF with Cu^{2+} at di□erent concentrations.

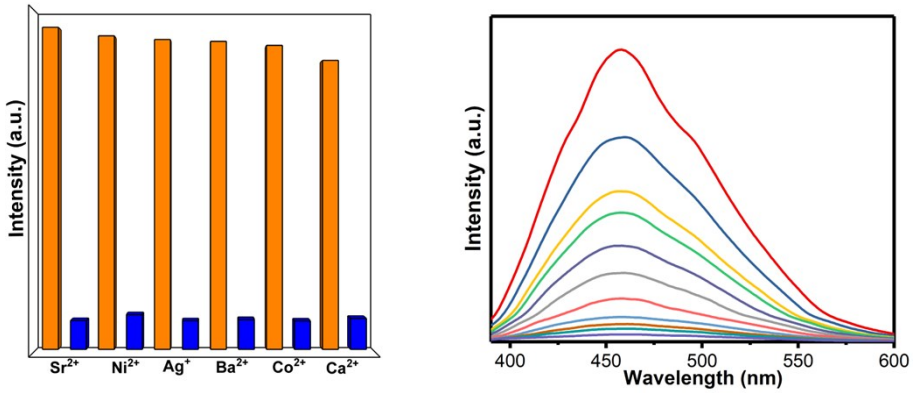

Fig. S8. (a) The effect of other metal ions on the fluorescence intensity of Cr^{3+}; (b) Fluorescence spectra of Cd-MOF with Cr^{3+} at di□erent concentrations.

1. C. H. Lin, J. D Chen and J. C Wang, Cryst. Growth. Des., 2008 **8** 1094.
2. V. Dolomanov, L. J. Bourhis and H. Puschmann, J. Appl. Cryst., 2009 **42** 339.
3. W. Zhang, R. Z. Zhang, Y. Q. Huang and J M Yang, Cryst. Growth Des., 2018 **18** 7533.
4. X. K. Yang, J. D. Chen, CrystEngComm., 2019 **21** 7437.
5. B. Dolenský, R. Konvalinka, M. Jakubek and V. Král, J. Mol. Struct., 2013 **1035** 124.